

Estimation of Direct Solar Radiation on High Mountain Region, Jomson, Nepal

Prakash M. Shrestha^{1,2}, Suresh Pd. Gupta^{1,*}, Usha Joshi^{1,2}, Narayan P. Chapagain³, Indra B. Karki¹, Khem N. Poudyal⁴

¹ Department of Physics, Patan Multiple Campus, Tribhuvan University, Nepal.

² Central Department of Physics, IoST, Tribhuvan University, Nepal.

³ Department of Physics, Amrit Campus, IoST, Tribhuvan University, Nepal.

⁴ Department of Physics, Pulchowk Engineering Campus, IoE, Tribhuvan University, Nepal.

* Corresponding e-mail: suresh.gupta@pmc.tu.edu.np

Abstract

The main aim of the study is to estimate direct solar radiation over high mountain region of Jomsom (Nepal) (28.47 °N, 83.83 °E, 2,700 m above sea level) for a period of year 2012. Aerosol optical depth (AOD) and total ozone column data are derived from NASA website. Daily atmospheric transmittance due to different parameters for direct solar radiation is calculated. The effect of different parameters on the direct solar radiation was analyzed. The maximum and minimum monthly average of direct solar radiation values were found $1208 \pm 22 \text{ W/m}^2$ in January and $1021 \pm 46 \text{ W/m}^2$ in June respectively. Annual average of direct solar radiation is $1106 \pm 70 \text{ W/m}^2$. Result of this research work is beneficial for the further identification, impact and analysis of direct solar radiation at different places, agriculture, energy harvesting.

Keywords: Air mass, Atmospheric transmittance, Ozone, Water contents, Solar radiation.

1. Introduction

Knowledge of the solar radiation arriving at the surface of the Earth is important for many different fields of study. Solar technology is one of the possibilities for on-site clean energy production as well as for the reduction of CO₂ emissions. Using photovoltaic (PV) panels, the incoming solar energy is transferred into electricity [1]. Sun is the closest star from the Earth and hence solar energy is the fundamental as well as primary source of energy. Sun radiates 4×10^{26} J energy per second. Sun emits electromagnetic wave of wavelength 300 nm to 3000 nm [2]. The clear sky model is essential in many specific application fields, like solar system design and estimation of solar energy technologies generation potential. As for the mountainous area with high altitude, due to the thin air and a few clouds, the clear-sky concept is more applicable [3,4]. Solar radiation decreases as square of distance from Sun to Earth. 1367 W/m^2 (I_{sc} , solar constant) [5]. Solar radiation incidents on the outer surface of Earth's atmosphere. Orbit of Earth around Sun is elliptical.

Solar radiation (I_0) incidents on specific point of outer surface of atmosphere at specific time depends on day number of year (DOY, n_d) [6].

$$I_s = I_{sc} \left[1 + 0.033 \cos\left(\frac{2\pi}{365} n_d\right) \right] \quad (1)$$

Solar radiation that passes through the earth's atmosphere to ground surface suffer scattering, reflection, and absorption by the atmospheric constituents like gas molecules, aerosols, water vapor, ozone and clouds. Solar radiation is attenuated in atmosphere with extinction coefficient (k) and optical air mass (m). Solar radiation is of two types, direct and diffused [7]. Solar energy is the largest renewable resources on earth. Study of direct solar radiation and its effect of different meteorological parameters are used in Agriculture, Hydrology, Climate change. Solar radiation depends on physical parameters such as attitude, longitude, altitude, optical air mass, aerosol, scattering, cloud, absorption, ozone, albedo and meteorological parameters such as precipitation, ambient temperature, wind speed, humidity, local weather conditions and seasonal variation [8]

Nepal is a mountainous land locked country located in the south east of Asia. Mountain is an important terrain type of the Earth's surface, according for approximately 24% of the global land surface [9]. Mountainous areas worldwide seem to have some common characteristics, such as lower temperature, inconvenient transportation which make mountainous areas highly vulnerable to the problem of energy poverty compared with plains [10]. Making full use of renewable energy on mountainous area is crucial. Due to the high altitude of the mountainous area, solar energy is abundant. Solar energy is also easy to obtain and nearly inexhaustible. Hence, solar energy is an ideal renewable energy source to be used in mountainous area with high altitude [11].

Nepal lies on Solar belt having latitude 15° N to 35° N and annual solar insolation varies from 3.6 to 6.2 kWh/m²/day [12]. Total consumption of energy in Nepal in fiscal year 2018/19 was 587TJ. Out of the total energy, conventional, commercial and renewable energy consumption were found as 68.5 %, 29.4 % and 2.1 % respectively [13]. Large amount of foreign currency is wasted on importing petroleum product. So energy harvesting from solar is required. The annual average solar energy measured in Biratnagar, Pokhara Kathmandu and Lukla are 4.95, 5.44, 5.19 and 4.61 kWh/m²/day respectively on the 26th January, 2010 [14].

Jomsom, Kingdom of Mustang, lies in the center of Mustang district of Gandaki Pradesh, western part of Nepal, having latitude 28.47°N, longitude 83.83° E being 2,700 m above sea level. The site, Jomsom, an administrative and commercial center with government officialssituated in between two famous mountains Nilgiri and Dhawalagiri. It is the district headquarters of the district having population of 1,370 [15]. The average high and low temperature of Jomsom is found in April 14° C and January -1° C respectively. The average rainy day is 104 and average rainfall is 659 mm. The average sun-shine hour is 7 hour.

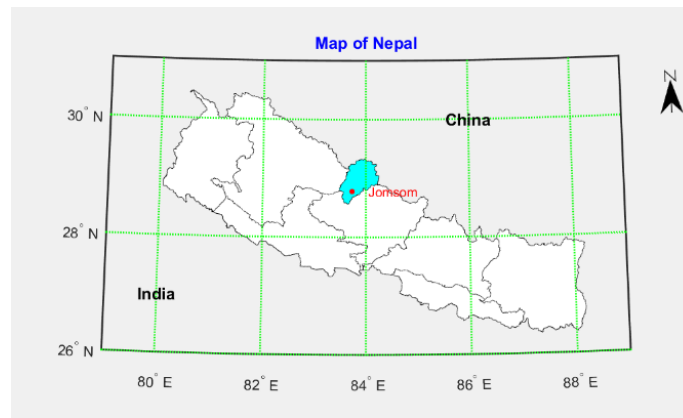


Figure.1: Map of Jomsom [source: Survey Department,2020]

Objective of study is to estimate direct solar radiation on Jomsom. There is no solar tracker to measure direct solar radiation in Nepal and estimation of direct solar radiation is required.

2. Materials and Methods

Atmospheric transmittance (τ) is ratio of solar radiation incidents on ground (I_B) to that incident on outer surface of atmosphere (I_o). According to Beer's law, atmospheric transmittance is defined as

$$\tau = e^{-k m} \tag{2}$$

Here k is known as extinction coefficient (k) which is sum of extinction coefficient due to presence of ozone (k_o), water vapor (k_w), gas mixture (k_g), aerosol (k_a) and Rayleigh scattering(k_r). So atmospheric transmittance is due to transmittance of Ozone(τ_o), transmittance of water vapor(τ_w), transmittance of gas mixture (τ_g), transmittance of aerosol (τ_a) and transmittance of Rayleigh scattering (τ_r) [16]. Here, τ_o depends on ozone column(l) and relative air mass (m_r). The relative air mass depends on zenith angle (θ_z), transmittance of water vapour (τ_w) depends on water content(w) and relative air mass and transmittance of gas mixture (τ_g), transmittance of Rayleigh scattering (τ_r) depends on air mass(m_a), atmospheric pressure(P), altitude and relative air mass. Transmittance of aerosol (τ_a) depends on Angstrom turbidity coefficient (β), Angstrom exponential(α) and air mass. These atmospheric transmittances are defined as [17].

$$\tau_o = 1 - [0.1611 u_3 (1 + 139.48 u_3)^{-0.8033} - 0.002715 u_3 (1 + 0.044 u_3 + 0.0003 u_3^2)^{-1}] \tag{3}$$

$$\tau_w = 1 - 2.4959 u_1 [(1 + 79.034 u_1)^{0.6892} + 6.385 u_1]^{-1} \tag{4}$$

$$\tau_g = e^{[-0.0127 m_a^{0.285}]} \tag{5}$$

$$\tau_a = (0.1244 \alpha - 0.0162) + (1.003 - 0.125 \alpha) e^{[-\beta m_a (1.099 \alpha + 0.6129)]} \tag{6}$$

$$\tau_r = e^{[-0.0903 m_a^{0.285} (1.01 + m_a - m_a^{0.64})]} \tag{7}$$

Where above other parameters are defined as (Kasten,1996)

$$u_2 = l m_r$$

$$u_1 = w m_r$$

$$m_a = \frac{P}{101325} m_r$$

$$m_r = \frac{1}{\cos \theta_z + 0.15(93.885 - \theta_z)^{-1.253}}$$

Bird and Hulstrom [18] developed a Parameterization Model C, called SOLTRAN and the direct solar radiation is given as

$$I_D = I_0 (0.9751 \tau_a \tau_w \tau_p \tau_o \tau_n + B(z)) \quad (8)$$

B(z) is a correction term for altitude, introduced by Bintanja [19] where z is altitude in meter.

The spectral aerosol optical depth (AOD) data of Jomsom for year 2012 was measured by CIMEL -318 sun photometer and are available in the AERONET homepage of NASA. The sun photometers multichannel radiometer measures direct solar irradiance. Here five wavelengths (λ) namely 675, 500, 440, 380 and 340nm are used to calculate Angstrom turbidity coefficient (β) and Angstrom exponential (α) by linear regression method. According to Angstrom model [20]

$$AOD = \beta \lambda^{-\alpha} \quad (9)$$

Total ozone column (TOC) is derived from NASA web site. Meteorological data are collected from website <https://www.weather-atlas.com>. Open source software Python 3.7 is used to analysis data and to plot graph. Standard error (SE) is used as error bar in the plotted graph. Data is presented in the form of mean (\bar{x}) \pm standard deviation(σ).

$$\sigma = \sqrt{\frac{1}{n} \sum_{i=1}^n (x_i - \bar{x})^2} \quad (10)$$

$$SE = \frac{\sigma}{\sqrt{n}} \quad (11)$$

Here n is number of data.

First quartile(Q1), second quartile(Q2, median) and third quartile(Q3) are 25%, 50% and 75% respectively of distribution of data. Skewness represents tailless of distribution of data. Zero skewness represent symmetric distribution. kurtosis gives density of distribution of data.

Zero kurtosis indicates normal distribution. Correlation coefficient (r) is used to find relation between two variables x and y. Its value lies between -1 to +1 and it is given as

$$r = \frac{\sum_{i=1}^n (x_i - \bar{x})(y_i - \bar{y})}{\sqrt{\sum_{i=1}^n (x_i - \bar{x})^2} \sqrt{\sum_{i=1}^n (y_i - \bar{y})^2}} \quad (12)$$

Coefficient of variance (CV) is used to check variability of data which is given as

$$CV = \frac{\sigma}{\bar{x}} \times 100 \quad (13)$$

Root mean square error (RMSE) and coefficient of determinant (R^2) are used to observe error using curve fitting.

$$RMSE = \sqrt{\frac{1}{n} \sum_{i=1}^n (y_i - \hat{y}_i)^2} \quad (14)$$

$$R^2 = \frac{\sum_{i=1}^n (y_i - \hat{y}_i)^2}{\sum_{i=1}^n (y_i - \bar{y})^2} \quad (15)$$

Here \hat{y}_i is estimated value of y .

3. Results and Discussion

With help of ozone column (l) and relative air mass (m_r), daily transmittance due to ozone (τ_o) are calculated by using equation (3). Figure.2(a) shows transmittance due to Ozone (τ_o). Its maximum value is 0.9885 in January 9 due to large value of total Ozone column (TOC) whereas minimum value is 0.9830 in July 14 due to less TOC. As stated all calculated data are form of mean \pm standard deviation. Annual average is 0.9864 ± 0.0016 . First quartile (Q_1) and third quartile (Q_3) are 0.9852 and 0.9878 respectively. Median (Q_2) is 0.9871. With the help of air mass (m_a), daily transmittance due to gas mixture (τ_g) are calculated by using equation (5). Figure.2(b) shows transmittance due to gas mixture (τ_g). Its maximum value is 0.9890 in February 16 whereas minimum value is 0.9876 in July 16 due to optical air mass. Annual average is 0.9885 ± 0.0004 . First quartile and third quartile are 0.9881 and 0.9890 respectively. Median is 0.9887. Daily transmittance due to water vapor (τ_w) are calculated by using equation (4) with help of water content (w) and relative air mass (m_r). Figure.2(c) shows transmittance due to water vapor (τ_w). Its maximum value is 0.9554 in January 6 whereas minimum value is 0.8757 in June 28 due to water content and optical air mass. Annual average is 0.9118 ± 0.0203 . First quartile (Q_1) and third quartile (Q_3) are 0.8941 and 0.9283 respectively. Median (Q_2) is 0.9130. Daily transmittance due to aerosol (τ_a) are calculated by using equation (6) with help of Angstrom turbidity coefficient (β), Angstrom exponential (α) and air mass (m_a). (Q_2) is 0.9322. Figure.2(d) shows transmittance due to aerosol (τ_a). Its maximum value is 0.9830 in June 13 due to large value to turbidity whereas minimum value is 0.7905 in February 27 due to less value of turbidity. Annual average is 0.9370 ± 0.0419 . First quartile (Q_1) and third quartile (Q_3) are 0.9213 and 0.9675 respectively. Median (Q_2) is 0.9515. Daily transmittance due to Rayleigh scattering (τ_r) are calculated by using equation (8) with help of air mass (m_a).

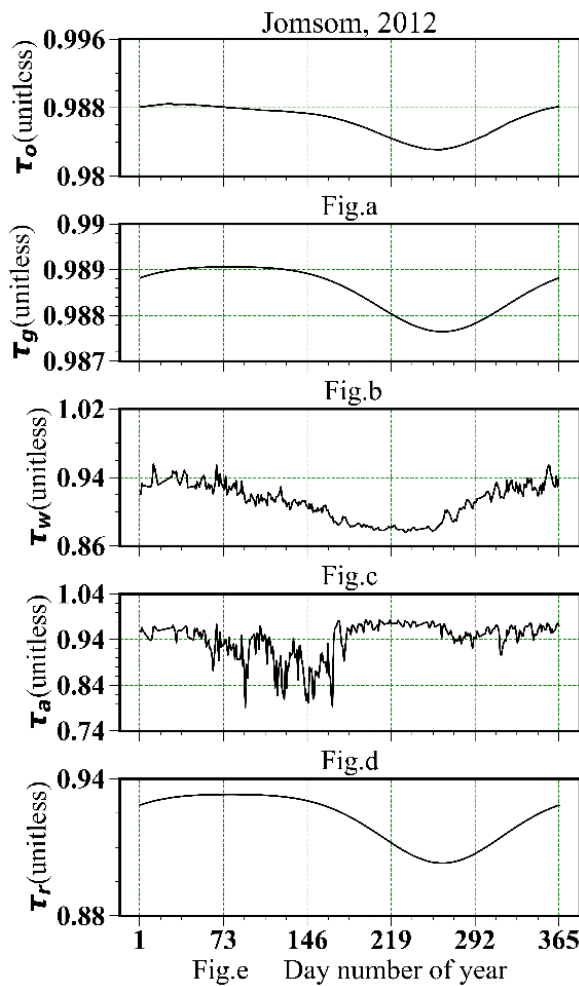


Figure.2: Daily Variation of atmospheric transmittance of Ozone, Gas mixture, Water vapor, Aerosol and Rayleigh scattering

Variation is large in spring due to 4% coefficient of variance and less in winter due to 2% efficient of variance. Figure.3(d) shows histogram of direct solar radiation. Skewness is -0.12. Distribution is negatively tailed. Kurtosis is -0.45. Peakness is small. It is not Gaussian distribution. 108 days has direct radiation between 1050 to 1150 W/m².

Figure.2(e) shows transmittance due to Rayleigh scattering (τ_r). Its maximum value is 0.9331 in February 16 whereas minimum value is 0.9030 in July 16 due to absolute air mass. Annual average is 0.9224 ± 0.0104 . First quartile (Q_1) and third quartile (Q_3) are 0.9135 and 0.9331 respectively. Median Daily direct solar radiation (I_B) are calculated by using equation (1),(3),(5),(6) and (7). Figure.3(a) shows daily variation of direct solar radiation (I_B). Its maximum value is 1242W/m² in June 30 due to less solar declination whereas minimum value is 907W/m² in May 11. First quartile (Q_1) and third quartile (Q_3) are 1066W/m² and 1167W/m² respectively. Median (Q_2) is 1092W/m². Figure.3(b) shows monthly variation of direct solar radiation. Its maximum value is 1208 ± 22 W/m² in January due to clear day whereas minimum value is 1021 ± 46 W/m² in June. Variation is large in April due to 5% coefficient of variance and less in August due to 0.5% coefficient of variance. Figure.3(c) shows seasonal variation of direct solar radiation. Its maximum value is 1201 ± 22 W/m² in winter whereas minimum value is 1050 ± 29 W/m² in summer.

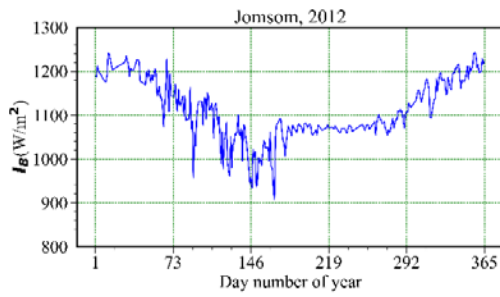


Figure 3a Daily variation of direct solar radiation

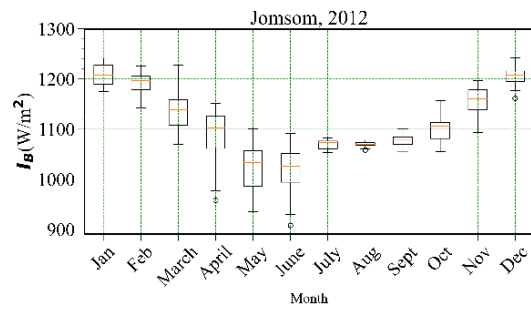


Figure 3b Monthly variation of direct solar radiation

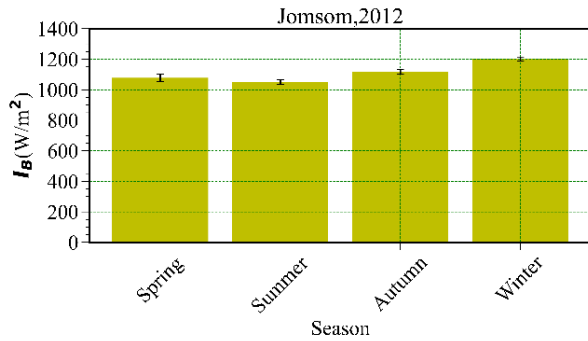


Figure 3c Seasonal variation of direct solar radiation

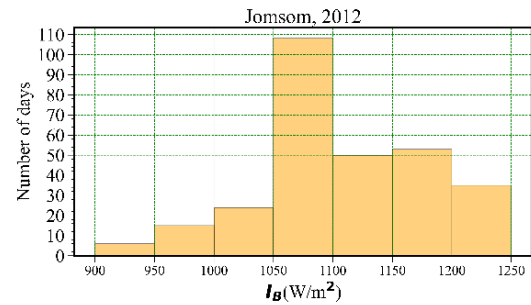


Figure 3d Histogram of direct solar radiation

Figure.3: Variation of Daily, Monthly, Seasonal and Histogram of solar radiation

Figure. 4(a) shows variation of direct solar radiation with maximum temperature. Annual average of maximum temperature is $5 \pm 6^\circ \text{C}$. Correlation coefficient is -0.86 . There is negative correlation. Figure.4(b) shows variation of direct solar radiation with minimum temperature. Annual average of minimum temperature is $-4 \pm 7^\circ \text{C}$. Correlation coefficient is -0.80 . There is negative correlation. Figure.4(c) shows variation of direct solar radiation with relative humidity (RH). Annual average of relative humidity is $69 \pm 16\%$. Correlation coefficient is -0.90 .

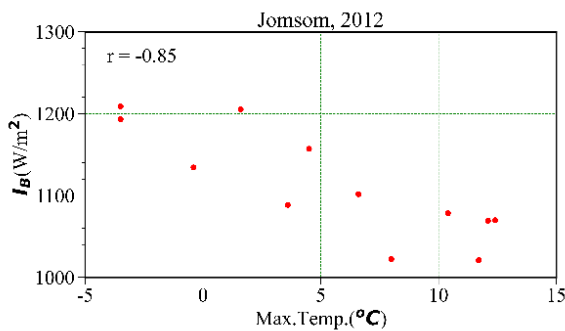
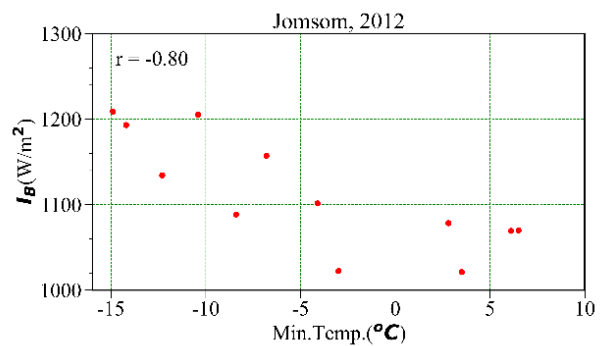


Figure 4a Variation of direct solar radiation



with monthly mean maximum temperature

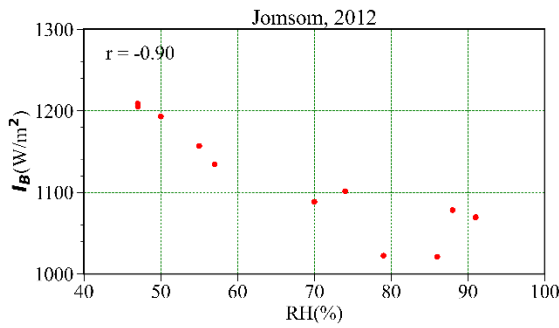


Figure 4c Variation of direct solar radiation with monthly mean relative Humidity

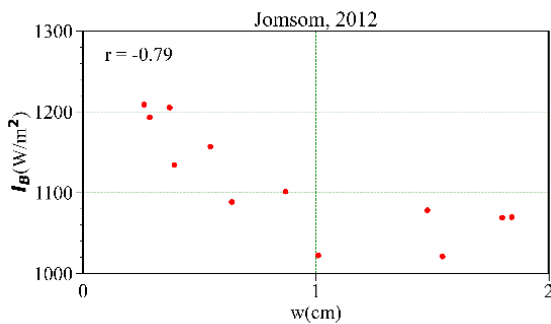


Figure 4e Variation of direct solar radiation with monthly mean water Content

Figure 4b Variation of direct solar radiation with monthly mean minimum temperature

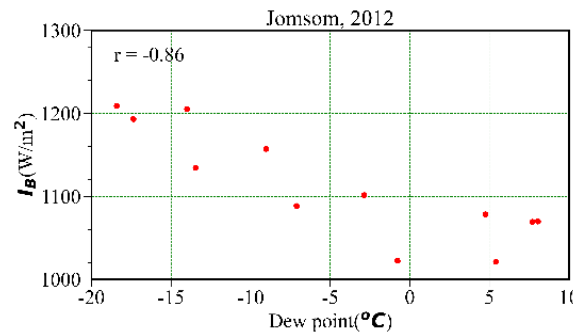


Figure 4d Variation of direct solar radiation with monthly mean dew Point

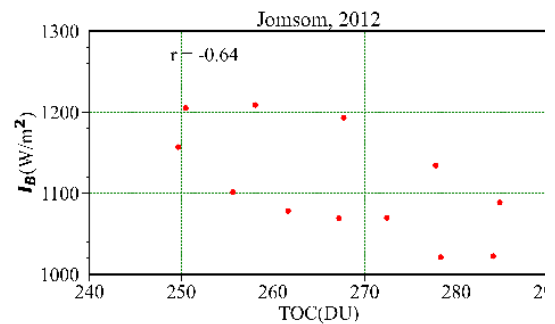


Figure 4f Variation of direct solar radiation with monthly mean TOC

There is negative correlation. Figure.4(d) shows variation of direct solar radiation with dew point. Correlation coefficient is - 0.86. There is negative correlation. Figure.4(e) shows variation of direct solar radiation with water content(w). Correlation coefficient is -0.79. Figure.4(f) shows variation of direct solar radiation with total ozone column (TOC). Annual average of relative humidity is 267 ± 1 DU. Correlation coefficient is -0.64. Figure.4(g) shows variation of direct solar radiation with ultraviolet index (UVI). Annual average of relative humidity is 9 ± 2 . Correlation coefficient is -0.89.

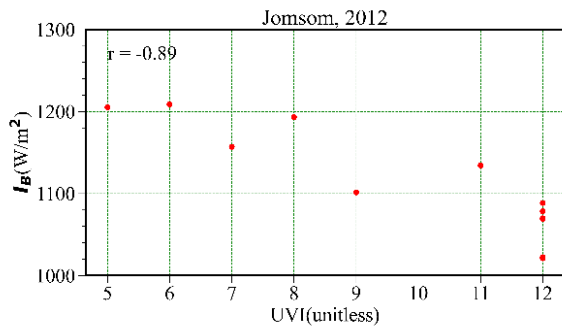


Figure 4g Variation of direct solar radiation with monthly mean UV

As mentioned above in figure 4, correlation coefficient with direct solar radiation with relative humidity is maximum. Straight line is fitted between direct solar radiation in W/m^2 and relative humidity in percentage as shown in Figure5. Straight line is

$$I_B = 1350 - 3 RH \tag{15}$$

Figure. 4: Variation of monthly mean direct solar radiation with maximum temperature, minimum Temperature, relative humidity, dew point water content, TOC and UVI

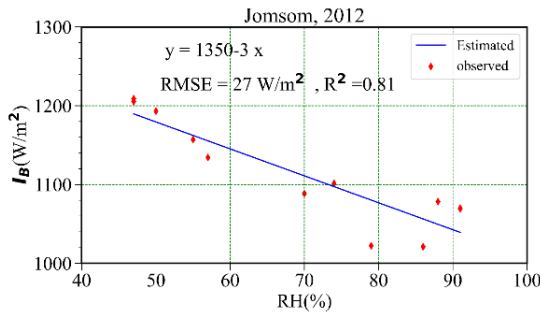


Figure 5 Curve Fitting between direct solar radiation and relative humidity

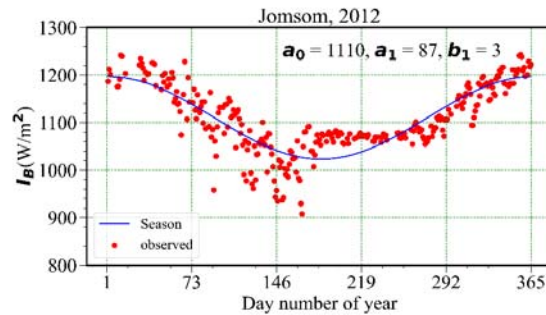


Figure 6 Fourier analysis of distribution of Solar radiation with days of the year.

Fourier series is used to analyze season variation. Figure.6 show model for direct solar radiation (I_B) in W/m^2 with day number of the year (n_d). Curve is

$$I_B = a_0 + a_1 \cos\left(\frac{2\pi}{366} n_d\right) + b_1 \sin\left(\frac{2\pi}{366} n_d\right)$$

$$I_B = 1110 + 87 \cos\left(\frac{2\pi}{366} n_d\right) + 3 \sin\left(\frac{2\pi}{366} n_d\right)$$

Offset is $1110 W/m^2$. Seasonal amplitude ($\sqrt{a_1^2 + b_1^2}$) is $87 W/m^2$.

4. Conclusion

Datasets on solar radiation is of great importance to the detection of global dimming and brightening. Direct solar radiation estimation is easily available satellite data on the basis of atmospheric transmittance and is important to propose solar radiation potential of the location, the sustainable development of ecological environments and agriculture based productivity. In study period of year-2012, annual average of direct solar radiation is found

as $1106 \pm 70 \text{ W/m}^2$. Direct solar radiation is more affected by relative humidity. There is linear relationship between direct solar radiation and humidity with RMSE of 27 W/m^2 and R^2 being 0.81. Model for direct solar radiation is developed on the basis of Fourier series with RMSE of 33 W/m^2 and R^2 is 0.72.

Acknowledgment

The authors would like to convey our gratitude to faculty of CDP, Patan Multiple Campus, IoST for this opportunity as well as NASA for the data. We sincerely appreciate NAST for the PhD fellowship. We also like to acknowledge Nepal Physical Society (NPS) and Association of Nepali Physicists in America (ANPA) for educational workshop of Python.

References

- [1] Agugiaro, G., Nex, F., Remondino, F., De Filippi, R., Droghetti, S., & Furlanello, C. (2012). Solar radiation estimation on building roofs and web-based solar cadastre. *ISPRS Ann. Photogramm. Remote Sens. Spat. Inf. Sci*, 1, 177-182.
- [2] Poudyal, K. N., Bhattarai, B. K., Sapkota, B. K. and Kjeldstad, B. (2012). Estimation of global solar radiation using clearness index and cloud transmittance factor at trans-himalayan region in Nepal. *Energy and power engineering*, 4(06):415.
- [3] Engerer, N. A., & Mills, F. P. (2015). Validating nine clear sky radiation models in Australia. *Solar Energy*, 120, 9-24.
- [4] Sun, X., Bright, J. M., Gueymard, C. A., Acord, B., Wang, P., & Engerer, N. A. (2019). Worldwide performance assessment of 75 global clear-sky irradiance models using principal component analysis. *Renewable and Sustainable Energy Reviews*, 111, 550-570.
- [5] Duffie, J. A. and Beckman, W. A. (2013). *Solar engineering of thermal processes*. John Wiley & Sons. Iqbal, M. (1983). *An introduction to solar radiation*. New York: Academic Press.
- [6] Liou, K. N. (2002). *An introduction to atmospheric radiation*, volume 84. Elsevier.
- [7] Salby, M. L. (2012). *Physics of the Atmosphere and Climate*. Cambridge University Press.
- [8] Kapos, V., Rhind, J., Edwards, M., Price, M. F., & Ravilious, C. (2000). Developing a map of the world's mountain forests. *Forests in sustainable mountain development: a state of knowledge report for 2000. Task Force on Forests in Sustainable Mountain Development*, 4-19.
- [9] Papada, L., & Kaliampakos, D. (2016). Developing the energy profile of mountainous areas. *Energy*, 107, 205-214.
- [10] Xu, L., Long, E., Wei, J., Cheng, Z., & Zheng, H. (2021). A new approach to determine the optimum tilt angle and orientation of solar collectors in mountainous areas with high altitude. *Energy*, 237, 121507.

-
- [11] Shrestha, J N., Bajracharya, T R., Shakya, S R. and Giri, B. (2003). Renewable energy in Nepal-progress at a glance from 1998 to 2003. *Proceedings of the International Conference on Renewable Energy Technology for rural Development (RETRUD-03)*, pages 12–14.
- [12] MoF (2018). *Economic Survey 2018/019*. Ministry of Finance, Government of Nepal.
- [13] Poudyal, K N., Bhattarai, B K., Sapkota, B K. and Kjeldstad, B. (2011). Solar radiation potential at four sites of Nepal. *Journal of the Institute of Engineering*, **8(3)**:189–197.
- [14] CBS. (2011). *National population and housing census 2011*, Central Bureau of Statistics, National Planning Commission Secretariat, Government of Nepal.
- [15] Iqbal, M. (2012). *An introduction to solar radiation*. Elsevier.
- [16] Bird, R. and Hulstrom, R. L. (1980). Direct insolation models. Technical report, *Solar Energy Research Inst.*, Golden, CO (USA).
- [17] Kasten, F. (1996). The Linke turbidity factor based on improved values of the integral Rayleigh optical thickness. *Solar energy*, **56(3)**:239–244
- [18] Bird, R. E. and Hulstrom, R L (1981). Simplified clear sky model for direct and diffuse insolation on horizontal surfaces. Technical report, *Solar Energy Research Inst.*, Golden, CO (USA).
- [19] Bintanja, R. (1961.) The parameterization of shortwave and longwave radiative fluxes for use in zonally averaged climate models. *Journal of climate*, **9(2)**: 439–454.
- [20] Angstrom, A. (1961). Techniques of determining the turbidity of the atmosphere. *Tellus*, **13(2)**:214–223.